Design of a visible-light spectroscopy clinical tissue oximeter

David A. Benaron
Stanford University School of Medicine
Department of Pediatrics
Division of Neonatal and Developmental Medicine
Palo Alto, California 94305
and
Spectros Corporation
Portola Valley, California 94028

Ilian H. Parachikov
Spectros Corporation
Portola Valley, California 94028

Wai-Fung Cheong
Stanford University School of Medicine
Department of Pediatrics
Division of Neonatal and Developmental Medicine
Palo Alto, California 94305
and
Spectros Corporation
Portola Valley, California 94028

Shai Friedland
Palo Alto and Livermore V. A. Medical Centers
Department of Gastroenterology
Palo Alto, California

Boris E. Rubinsky
David M. Otten
University of California at Berkeley
Department of Mechanical Engineering
Berkeley, California

Frank W. H. Liu
Stanford University School of Medicine
Department of Pediatrics
Division of Neonatal and Developmental Medicine
Palo Alto, California 94305
and
Spectros Corporation
Portola Valley, California 94028

Carl J. Levinson
Stanford University School of Medicine
Department of Obstetrics and Gynecology
Palo Alto, California 94305
and
Spectros Corporation
Portola Valley, California 94028

Aileen L. Murphy
John W. Price
Yair Talmi
James P. Weersing
Joshua L. Duckworth
Uwe B. Hörchner
Eben L. Kermit
Spectros Corporation
Portola Valley, California 94028

Address all correspondence to Dr. David Benaron, Spectros Corporation, 4370 Alpine Road, Suite 108, Portola Valley, CA 94028. Tel: 650-851-4040. Fax: 650-851-4099. E-mail: dbenaron@spectros.com. Web site: www.spectros.com.

Abstract. We develop a clinical visible-light spectroscopy (VLS) tissue oximeter. Unlike currently approved near-infrared spectroscopy (NIRS) or pulse oximetry (SpO_2%), VLS relies on locally absorbed, shallow-penetrating visible light (475 to 625 nm) for the monitoring of microvascular hemoglobin oxygen saturation (StO_2%), allowing incorporation into therapeutic catheters and probes. A range of probes is developed, including noncontact wands, invasive catheters, and penetrating needles with injection ports. Data are collected from: 1. probes, standards, and reference solutions to optimize each component; 2. *ex vivo* hemoglobin solutions analyzed for StO_2% and pO_2 during deoxygenation; and 3. human subject skin and mucosal tissue surfaces. Results show that differential VLS allows extraction of features and minimization of scattering effects, *in vitro* VLS oximetry reproduces the expected sigmoid hemoglobin binding curve, and *in vivo* VLS spectroscopy of human tissue allows for real-time monitoring (e.g., gastrointestinal mucosal saturation $69 \pm 4\%$, $n = 804$; gastrointestinal tumor saturation $45 \pm 23\%$, $n = 14$; and $p < 0.0001$), with reproducible values and small standard deviations (SDs) in normal tissues. FDA approved VLS systems began shipping earlier this year. We conclude that VLS is suitable for the real-time collection of spectroscopic and oximetric data from human tissues, and that a VLS oximeter has application to the monitoring of localized subsurface hemoglobin oxygen saturation in the microvascular tissue spaces of human subjects. [DOI: 10.1117/1.1979504]

Keywords: visible light; spectroscopy; oximetry; hemoglobin; saturation; *vivo*; near-infrared spectroscopy; visible-light spectroscopy; clinical; medical.

Paper 03052 received Apr. 24, 2003; revised manuscript received Jun. 18, 2004; accepted for publication Feb. 18, 2005; published online Aug. 15, 2005.

1 Introduction

There is a significant gap between the clinical potential of tissue oximetry[1–6] and its limited clinical adoption.[7–12] Tissue oximetry, unlike pulse oximetry, is sensitive to the inadequacies in local blood flow, called ischemia, that underlie clinical conditions such as stroke, heart failure, peripheral vascular disease, and many cases of organ failure. One might have expected this advantage to lead to widespread clinical use; however, clinical use of tissue oximetry remains rare.

We hypothesize that a limiting factor in the clinical adoption of tissue oximetry is the very use of near-infrared spectroscopy (NIRS) itself. The more recent medical device successes have tended to be invasive catheters that achieve a therapeutic benefit by acting internally and locally on small volumes of tissue [e.g., stents, cardiac and neurosurgery catheters, and thermal ablation probes. (Ablation is used clinically

1083-3668/2005/10(4)/044005/9/$22.00 © 2005 SPIE

to mean the killing of viable tissue. For example, the freezing of tissue is called cryoablation. This differs substantially from the physicist's use of the same term.)] In contrast, NIRS, the basis for all other tissue oximeters currently approved for clinical use in the United States,[13] relies on large-volume, deeply penetrating photons, emitted and detected using widely spaced sensors, to reach internal tissues such as the brain and leg muscle beds. In addition, the low extinction of near-infrared light by hemoglobin forces NIRS to use long tissue paths to generate a reliable, measurable absorption. Such factors make it difficult to deploy NIRS oximetry into such locally acting catheters, where we believe large and untapped clinical opportunities lie.

Based on this hypothesis, we turned away from the conventional wisdom of the near-infrared "optical tissue window," and instead looked to the visible spectrum. Our prior experience had been in developing imaging for living tissues using either external light sources,[14–17] or internal biological sources such as luciferase.[18–21] In particular, when our group proposed and then demonstrated the very first use of luciferase imaging *in vivo* in intact mammals, the approach had been widely expected to fail. The luciferase constructs available at that time operated at the blue end of the visible spectrum, wavelengths for which tissue was generally thought of as being completely opaque. The rapid and widespread adoption and commercialization of *in vivo* luciferase imaging approaches[22,23] suggested that other visible-light-based approaches might work as well.

We report development of a quantitative clinical tissue oximeter[24] suitable for use in small, locally acting probes, catheters, and needles, that is based not on NIRS, but on visible light spectroscopy (VLS). Validation of VLS oximetry in human subjects is reported in a companion article published in the clinical literature.[25]

2 Methods

2.1 *VLS Oximeter Design*

Key clinical design goals included: 1. quantitative microvascular hemoglobin oxygen saturation measurement, 2. the ability to operate embedded into therapeutic catheters, 3. clinical ease of use, and 4. fast response times facilitating interventional procedures.

We began with a laptop-based VLS system that optically characterized or classified living tissues using partial least-squares (PLS) analysis and a nonscanning spectrophotometer,[26] and optimized this system over four generations of instruments.[27] While such a nonscanning device is becoming the obvious approach today for the rapid analysis of signals *in vivo*, when first constructed, this approach was novel. Briefly, we configured a charge-coupled device (CCD) spectrophotometer to be visible-light sensitive. The detector (ILX511 linear sensor, Sony, Japan) consisted of a 2048-element array with a 12.5-μm width (14 μm center to center) by 200-μm pixel area. Unused leading and trailing bins were masked to estimate dark count and offset voltage at each integration time (5 ms to 1 s). Sensitivity was 0.03 fJ per count at 600 nm (1 count/86 incident photons/pixel), but this fell to 1 count per 50,000 photons when accounting for fiber coupling (35%), grating efficiencies (70%), and photon capture (0.6% efficiency for multiply-scattered light into a 12-deg fiber-capture half angle). This yielded linear photon counts from 2 pW to 16 nW incident on the detector fiber.

The resulting clinical system was designed to meet United States [e.g., Food and Drug Administration (FDA)[28,29]] and European Union (e.g., CE mark[29,30]) medical device requirements, including software[31,32] and device[33] guidelines for mitigation of hazards, design control, verification, validation, biocompatibility, manufacturing, and safety. Manufacturing was transferred to an FDA-certified assembly facility. FDA approved VLS systems began shipping earlier this year.

2.2 *Analysis Software*

Spectral standards were provided in software-readable Windows® INI files. For oximetry, hemoglobin standards were provided (oxy, deoxy, and met species). Integer wavelength alignment of collected spectra corrected for grating differences between systems. Standards were then used to solve for the concentration of each standard spectrum in the tissue using a scatter-corrected least-squares matrix fit on native or differential measured spectra. Iterative feature stripping allowed for complex analysis (e.g., solving for hemoglobin at one wavelength range, then solving chemotherapy drugs at another). Error checking allowed abnormalities to be detected (e.g., known abnormal hemoglobin in trial fits, or unknown spectral contaminants causing excessive fit residuals).

Data processing was governed by a readable INI file, written in a custom macro language script. In the oximeter, analysis is based on first differential spectroscopy, with a fit of scattering and absorbance from 476 to 586 nm. Calculation of absorbance, filtering, derivative calculation, and fitting were performed in real time, and required 30 ms per averaged spectrum set using an embedded single board computer.

Use of INI files for both standards and processing allows the VLS system to be user configured as required for tissue oximetry, tissue identification or characterization, or parametric probe guidance during interventional procedures, all using the same validated core software kernel. Examples of alternative analysis include the identification of chemotherapy agents such as Doxorubicin or Tirapazamine,[34] probe guidance for targeted injection of therapeutic substances, and monitoring of localized nonsurgical tissue ablation.[35,36]

For research use, a password-protected operating mode allowed standards and scripts to be modified, and data to be saved to an internal flash memory and later exported in Microsoft Excel-compatible form via the external USB port. Because an oximetry system with modified standards or scripts must never be confused with validated clinical oximeters, a self-test detects user-altered systems and prominently indicates at startup that the software has been modified, and that the device is for "research use only."

2.3 *Light Source Development*

There are significant drawbacks to the bulb sources typically used for broadband optical spectroscopy. Unlike narrow, coherent sources such as lasers, broadband sources are difficult to couple to a biological sample. They tend to emit light over a wide spherical angle from nonpoint sources, rendering inefficient attempts to direct their light either onto tissue samples or into fibers, and they tend to run hot, discouraging close approximation to living tissue.

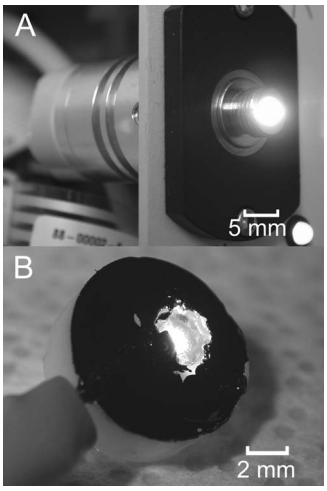

Fig. 1 Light sources developed. (a) A small but intense light source developed under SBIR support produces 3.5 W/cm^2. The device measures $25 \times 25 \times 38$ mm and requires no cooling fan. (b) A broadband, low-thermal-transfer LED light source deployed into the tip of the probe itself, delivering a similar intensity of illumination for much less power and lowered local heating of the sample.

For illustration, consider a 1-cm filament bulb. The bulb's surface area is 105 mm^2, while the area contacting a 1-mm tissue sample placed against the glass is only 0.8 mm^2. Thus, the target tissue intercepts less than 1% of the bulb's visible light output. In practice, because this bulb is hot, a fiber is required to transmit the light to the tissue. When accounting for both the low conversion efficiency of input energy to visible light (about 4% for conventional bulbs) and the poor transfer of light to tissue via a 100 μm fiber, only 0.0003% of the energy flowing into this bulb ends up transmitted to the tissue—equivalent to 333 W of input energy required for each mW of visible light delivered. To address this issue, we developed two miniaturized light sources.[37]

First, we developed a high-intensity fiber-coupled halogen source [Fig. 1(a)]. In this system, an integrated lens in the light bulb housing, placed only a few millimeters away from the filament, couples light into a collimated beam, while a reversed beam expander (NA 0.55, FL mm) separated by an air gap from the bulb for thermal isolation, focuses the light in a collimated beam directly onto the fiber face. Reducing the distance from the filament to the lens allowed use of a shorter focal length and higher NA lens, enabling the fiber to intercept a larger fraction of the emitted light.

Second, we developed a white LED source for integration directly into the probe itself for high light coupling with low transmission losses [Fig. 1(b)]. Because a broadband LED emits primarily in the desired band, it runs more efficiently, allowing for cool operation and close juxtaposition of the tissue and source. This proximity, in turn, further raises the efficiency of light transfer, as a narrow-aperture coupling fiber is no longer required. An LED also allows for an inexpensive electrical connection of the bulb to the monitor, rather than a fiber coupling, or even for no electrical connection at all if a disposable power source is embedded in the probe.

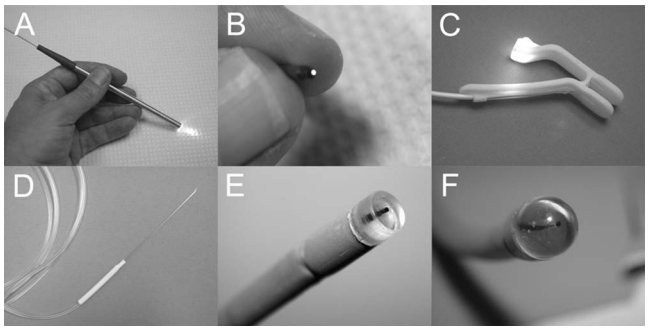

Fig. 2 Clinical probes used in human trials. Application-specific VLS oximetry probes, including (a) a 6×200-mm hand-held wand, (b) a 2-mm-diam endoscopic catheter, (c) a clip-on buccal probe, (d) a 27-Ga needle probe, (e) a 5-mm-diam esophageal monitoring catheter, and (f) a 12-mm-diam flexible colonic probe used here for human gastrointestinal studies.

2.4 *Probe Design*

A goal of probe design was interchangeability, allowing different therapeutic catheters and probes to be attached to the oximeter. Early probe designs[27] were refined and reduced to a reproducible set of application-specific clinical probes for human use. These probes include a 6×200-mm hand-held wand constructed for neurosurgical, plastic, cardiac, and vascular surgery applications, used here for skin studies [Fig. 2(a)]; a 2-mm-diameter endoscopic catheter designed for invasive studies, used here for human gastrointestinal mucosal studies [Fig. 2(b)]; a clip-on probe designed for buccal placement [Fig. 2(c)]; a 27-Ga needle probe developed for tumor oximetry and chemotherapy level estimation [Fig. 2(d)]; a 5-mm-diameter esophageal monitoring catheter, used here in human gastrointestinal studies [Figure 2(e)], and a 12-mm-diameter flexible colonic probe, used here for human gastrointestinal studies [Fig. 2(f)]

2.5 *Calibration Standards*

2.5.1 *Hemoglobin standards.* Hemoglobin absorbance values were assembled from the literature[38–40] to form a standard hemoglobin dataset. These spectra can be downloaded at our web site (www.spectros.com). We compared published spectra to spectra we measured *in vivo* and *in vitro*. Differences between these spectral sets were not significant under differential analysis, as shown by oximetry tests in which the mean saturation difference was 0.6% using one spectral set as compared to the other in analysis of the hemoglobin solution, described later.

2.5.2 *Calibration sets.* We developed calibration caps of known optical characteristics for each probe. We evaluated five standardization methods reported previously: 1. calibrated intralipid solution (with or without added broadband carbon absorber or water-soluble dyes),[41] 2. hard Delrin or resin blocks[42] with holes for inserting the needle probes (with and without coupling fluids), 3. soft siloxane[43] or room-temperature vulcanized (RTV) silicone rubber mixtures[44] with added titanium dioxide scatterer and carbon power absorber, 4. paper fibers, and 5. commercial flat-white reflectance stan-

dards. The reflectance, stability, flatness, and reproducibility of these standards were measured and compared.

2.6 *Ex Vivo Methods*

2.6.1 *Dye concentration tests.* Two dyes were utilized: a red dye 40 and 3 mixture, and a red dye 40 and blue dye 1 mixture (Shilling, McCormick and Company, Hunt Valley, Mayland). Dyes were added singly or as a ratiometric pair to solutions to produce a peak absorbance of 0.005 to 0.025/mm in clear solution. Because VLS probes were designed to work in scattering tissue, 20% LipoSyn™ was added to the dye solution for a final concentration of 1 to 4% v/v lipid/water. Data were analyzed for the effect of scattering on apparent dye absorbance, and for the variation between actual and calculated dye concentrations.

2.6.2 *Hemoglobin solution.* Blood was drawn from healthy volunteers into heparinized vials. Samples were spun at 1500 G $\times$ 10 min, the serum supernatant withdrawn, and the cell pellet resuspended in 0.9-M saline $\times$ 2 spin and wash cycles. After the third spin-down, cells were then resuspended in distilled water. After allowing 15 min for cell lysis, the sample was spun down, and any material pellet was left behind after transfer to a new vial. The resulting solution was bright red, transparent, and without noticeable light scattering. Hemoglobin concentration was estimated by transmission spectrophotometry. The solution was diluted to 50 μM in pH 7.4 buffered saline to match a reasonable estimate for blood content in tissue (using the peak absorbance of a well-oxygenated solution at 576 nm, ε=0.0139/cm/μM). The visible spectrum was recorded.

2.6.3 *Deoxygenation of free hemoglobin.* For *in vitro* deoxygenation, a 125-ml flask with stir bar was filled with the previous hemoglobin solution. An oxygen electrode (Model 2100, VWR, West Chester, Pennsylvania) was inserted through a sealed cork, along with a pop-off vent for CO_2 production, a needle probe, and a pH meter probe. All probe insertion sites were made air tight using a silicone-based vacuum gel sealant and ParaFilm™. The flask was placed on a magnetic stirring plate. 20% LipoSyn™ was added to the hemoglobin solution for a 1:10 final dilution of the lipid, or 2% weight/volume lipid. The pH was initially adjusted to 7.40 using 0.01 M NaOH. The visible spectrum was recorded.

To force hemoglobin deoxygenation in a gradual manner, we used the procedure of Chance et al.[45] in which 1-mg active dry yeast and 5-mg table sugar were mixed in 2-cc warm water, and this slurry was added to the hemoglobin solution. The yeast did not alter the oxygenated spectrum (data not shown). Spectra were continuously measured during deoxygenation on a stir plate, until the spectra were stable and did not change. The pO_2 was continuously recorded for cross referencing during data analysis; pH was measured but not adjusted during deoxygenation. Deoxygenation required 1 h. Saturation was calculated and compared to published sigmoidal hemoglobin oxygen binding curves.

Fig. 3 Buccal probe on adult cheek. The white LED light illuminates the inner mucosal side of the cheek.

2.7 *In Vivo Methods*

VLS oximetry was recorded using the clinical probes at one or more sites in each subject from the skin, and from mucosal surfaces in the cheek, esophagus, stomach, intestine, and/or colon.

First, surface oximetry was performed on skin in a series of noninvasive measures on the skin. Hand measurements from a Caucasian, the dorsal surface of an African American, the ear lobe of a Caucasian, and the lip of a Caucasian were obtained using the wand probe [Fig. 2(a)].

Second, mucosal oximetry was measured in a series of nonpenetrating, reflection measurements of the inner surface of the gastrointestinal tract during a routine endoscopic exam. Endoscopic measures were collected after Institutional Review Board (IRB) review, Human Studies approval, and with written informed consent. Measurements were made using the clinical endoscopic VLS catheter [Fig. 2(b)] or rectal catheters [Figs. 2(e) and 2(f)] held a few millimeters away from the mucosal surface.

Third, buccal oximetry was measured from the inner surface of the cheek during planned cardiac arrest during cardiac repair. Buccal measures were collected after IRB review, Human Studies approval, and with written informed consent. Measurements were made using the buccal VLS clip [Fig. 2(c)], as shown on a human subject (Fig. 3). The percentage of time during which the tissue oximeter and the pulse oximeter collected data during cardiac surgery was monitored. Because there are periods during which there is no pulse, up time was determined as the percentage of 5-s windows during which at least one valid oximetry signal was recorded.

The goal of these *in vivo* tests was to demonstrate that the expected VLS spectral features were seen in living subjects, thus confirming that VLS accurately records spectroscopic information from human subjects. Validation of VLS oximetry measurements in a large population of patients is reported in a companion article (see discussion).

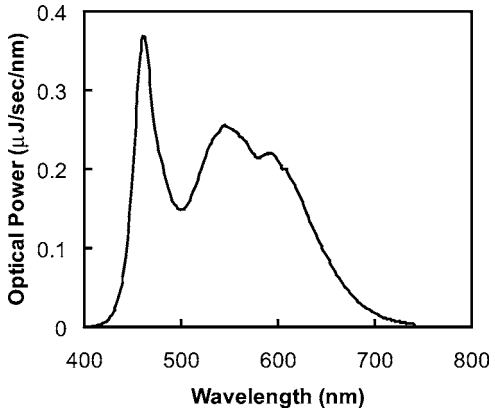

Fig. 4 Output of the phosphor-coated blue LED. Power is measured as per the ANSI standard test for eye safety for light emitting devices, in which the light is passed through a 3.5-mm slit and measured at 100-mm distance. The peak emission from the blue LED is visible at 463 nm, while the phosphor produces an overlapping broadband peak extending the range of illumination to more than 700 nm.

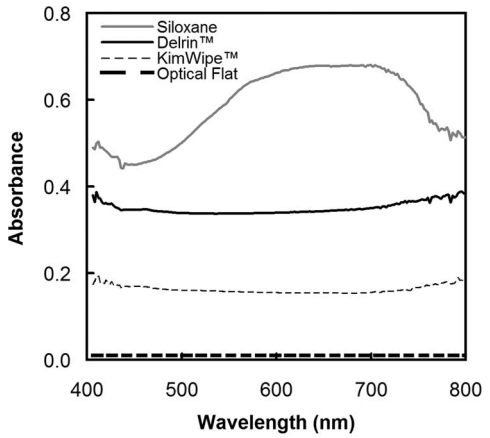

Fig. 5 The spectral flatness of the reference materials tested. Absolute reference is an optically flat NIST-traceable diffuse spectral standard. All other standards demonstrate a degree of spectral response. Small-fiber paper standards, such as thick, quantitative filter paper or commercial dust-free wipes, were the most consistent, easily made standards.

3 Results

3.1 *Hardware Performance Results*

3.1.1 *Light source performance.* Halogen lamp source visible light intensity was captured and measured using a 100-μm fiber either directly coupled to the bare bulb (3.4 to 7.5 mW/mm^2) or coupled through an integral lens in the bulb (67 to 152 mW/mm^2; 1.20 mW peak total). Incorporation of an integral lens, inside the bulb and close to the filament, allowed for a 10 to 45 fold improvement in light collection.

The cool LED light illumination of tissue was measured using illumination either captured and delivered through a 100-μm fiber (0.37 mW delivered to the tissue) or by direct LED illumination of the tissue after placement of the LED into the tip of a medical instrument (3.2 mW delivered to tissue). The spectrum of light measured when embedded into the buccal probe is shown in Fig 4. Direct coupling of the cool source increased light delivery to the tissue by 10 fold. This exceeded the visible light delivery from the lens-coupled halogen bulb by 3 fold, despite a much lower light density of the LED source, due to the larger effective aperture achieved through direct illumination.

3.1.2 *Probe performance.* Returning light levels for the end-emitting needles [Fig. 2(d)] was 56 nW in 2% IL, or about 0.01% of the transmitted input fiber light of 520 μW (67 mW/mm^2 into a 100-μm core fiber). Throughput for the optical forceps varied with separation thickness, but was not detectable for tissue thicknesses of 1 cm or greater. Cross talk varied significantly by probe configuration. End-emitting needle probes were susceptible to significant cross talk in air, from 0.01% to more than 1% of total input signal, typically from scattering through the cladding at the needle end. Side-emitting, fiber array, and forceps probes had little or no detectable cross talk. Cross talk was best reduced by the use of dense black epoxy potting material as well as by the presence of a metallic barrier between the fibers.

2.1.3 *End angle polish.* Medical needles tend to be sharp, with narrow end angles to facilitate tissue penetration with minimum local blunt trauma. However, light exiting the fiber in tissue was substantially diminished due to internal reflection when the angle of the tip was less than 30 deg, even when in contact with moist tissue (refractive index about 1.36) rather than air (index=1.00). This is likely due to the high refractive index of the optical fibers (n=1.46 to 1.50). Because of this, sharp polishing to a medical angle of 15-deg results may not be practical.

3.2 *Standards*

3.2.1 *Reflectance standards and probe calibration.* The spectral flatness and total reflectance of the tested standards varied widely (Fig. 5). Some standards exhibited spectral fea-

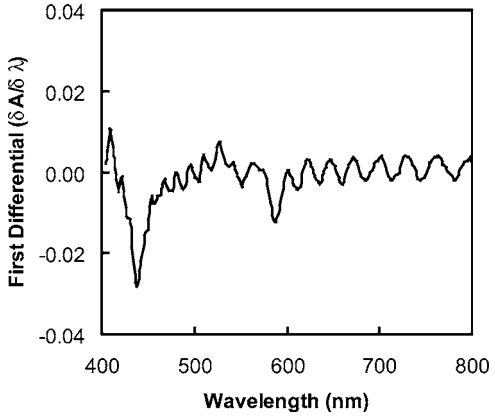

Fig. 6 Oscillations from liquid Intralipid-based standards. Use of Intralipid solutions for reference scattering for the needle probes at times produced wavelike variations in the reference curves, consistent with Mie-theory variations in some studies. These oscillations were most notable after differential spectroscopy, and introduced error into the quantitation of concentration. As a result, we discontinued use of liquid standards for the VLS calibration.

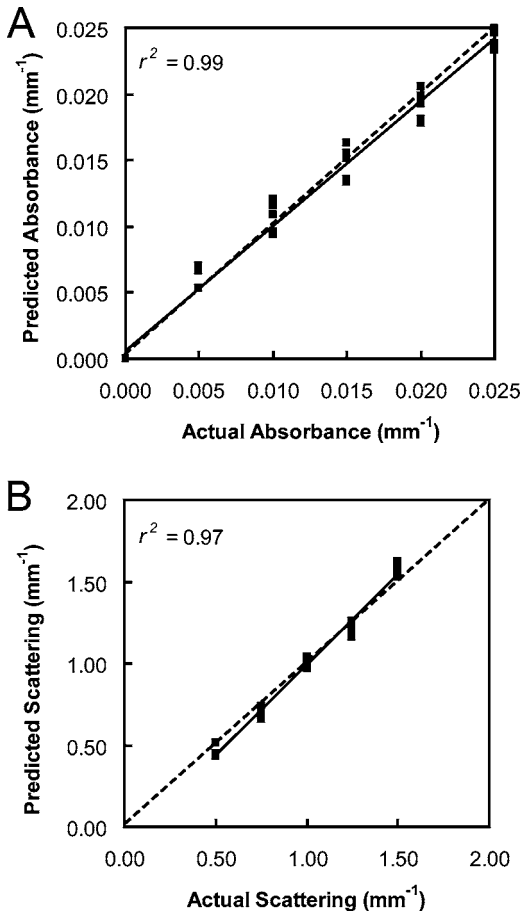

Fig. 7 Predicted versus actual absorbance and scattering plots. Scatter- and differential-corrected plots for measured (a) absorbance and (b) scattering are shown for a range of lipid and dye concentrations intended to cover the physiologic range of expected values in tissue *in vivo*. The line of identity is shown as a dashed line in each plot.

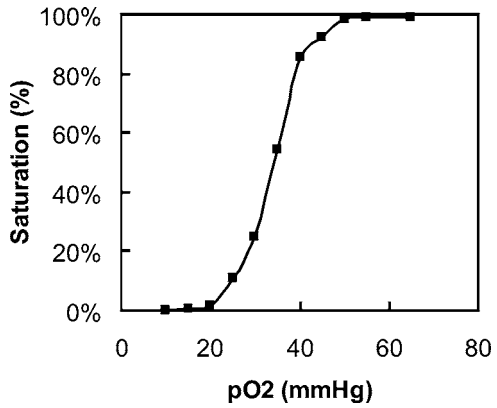

Fig. 8 Deoxygenation binding curve as measured using VLS. The measured p50 (the point at which 50% of the hemoglobin is saturated with oxygen) is 35-mm Hg. The expected p50 for human hemoglobin is 33±2-mm Hg under the conditions of pH 6.6, no 2,3-DPG, pCO_2 =0.6-mm Hg, and 20° C.

tures (such as water and fat features in the intralipid standard above 900 nm, or the 912-nm feature in the silicone standard). The noncontact and surface-contact probes were best calibrated using dully surfaced diffuse reflectance materials, which reduced specular reflections, allowed the angle of measurement to be of low importance in the standardization, and exhibited good reproducibility of the reflected intensity.

The invasive needle probes, unlike surface contact probes, demonstrated large variations in coupling to solid standards, with returning light intensity for a given probe showing a repeated measure variation (1 SD) of 12.8% of mean intensity. Liquid standards produced less variation (0.2% of mean intensity). However, lipid-based aqueous standards also produced unpredictable wavelike variations in the reference curves (Fig. 6), especially after the lipid samples were left standing. These oscillations, attributable to Mie-like scattering effects, introduced error into the reference spectrum, which then carried into clinical measurement. This error was unacceptably high when testing for low-concentration compounds such as chemotherapy agents, or when using higher-order differential spectroscopy. In contrast, the soft solid polysiloxane-based standards did not exhibit such similar oscillation, but exhibited a return intensity that varied with needle pressure. Polysiloxane coupling variability was reduced using a consistent compressive force between the standard and the probe (0.3 to 0.6 N), and by lowering the scattering coefficient of the standard. Such intensity-related measures would be of less importance in approaches that are not intensity based (e.g., frequency and time-domain measures). Last, the addition of a small amount of dye to the standard allowed for estimation of volume measured.

3.2.2 *Dye.* The spectral effects introduced by scattering were reduced by use of differential spectroscopy.[46] In the absence of a scattering correction, the match between the unscattered and noncontact scattering waveform spectral errors improved using differential spectroscopy, which emphasizes nonlinear effects over the baseline offset and exponential effects induced by scattering and variations in the coupling. When further including a scattering correction in the fitting method, calculated dye concentration was independent of scattering over a wide range of scattering levels (scattering 0.5/mm to 1.5/mm (r^2=0.97), absorbance 0.005 to 0.025/mm [r^2=0.99], Fig. 7). A ratio of the measured concentration of two dyes, a model for the determination of saturation used in tissue oximetry, was independent of scattering over the range of scattering coefficients seen in most tissues (ratio =0.550±0.020, or a variance of 3.6%). This suggests that ratiometric measures, such as hemoglobin saturation, should be stable and independent of the tissue monitored *in vivo*.

3.2.3 *Hemoglobin.* The measured spectra of oxygenated and deoxygenated hemoglobin compare well to published values. Spectral peaks agree with a mean difference of 1.0±0.8 nm (HbO_2 peaks measured at 543 and 578 nm versus published values of 542 and 578 nm, Hb peaks measured at 557 nm versus published values of 556 nm). These differences became insignificant using differential spectroscopy. A plot of calculated hemoglobin saturation versus measured electrode pO_2 demonstrates an oxygen dissociation curve with the expected sigmoid shape (Fig. 8) and good p50 agreement

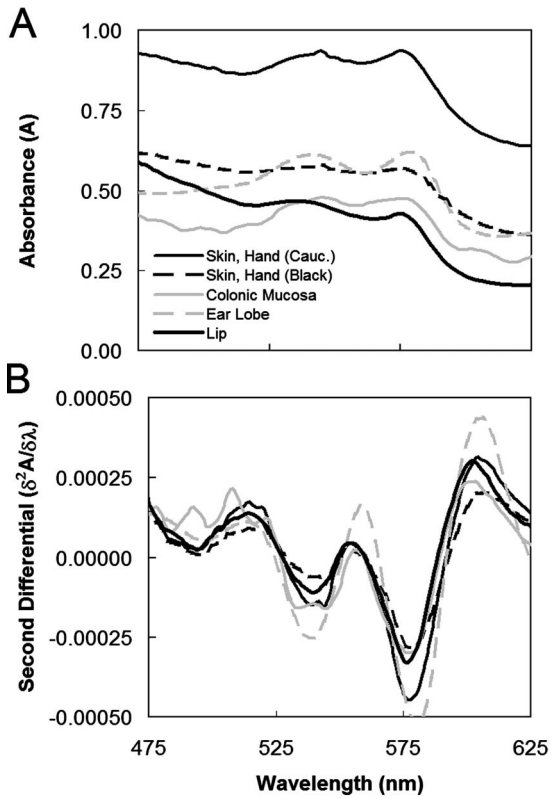

Fig. 9 Differential spectroscopy applied to *in vivo* spectra. (a) Absorbance plots show differing baseline and slope in human tissues measured *in vivo*. (b) Second differential plots remove much of this baseline variation, and enhance the nonlinear spectral features, such that the hemoglobin peaks from different tissues substantially overlap. Note the 480- to 520-nm feature in the colonic mucosal spectrum seen more clearly in the differential plot.

with values published in the literature[38] (p50 measured =35-mm Hg, p50 expected=33±2-mm Hg under the conditions of pH 6.6, no 2,3-DPG, and 20°C).

3.3 *In Vivo Spectrophotometry*

The spectral signals recorded from noninvasive measures on the hand of a Caucasian subject, the dorsal hand of an African American subject, on the ear lobe of a Caucasian subject, the lip of a Caucasian subject, and the colonic mucosa of a human subject undergoing endoscopy are shown in Fig. 9(a). Each spectrum required between 25 to 45 ms to collect. The signals show substantial variation in absolute reflectance intensity, background scattering, and hemoglobin signal strength. A fit assuming the presence of adult hemoglobin plus scattering accounted for the most of the observed spectral shape (mean rms fit error=2.7%). Background variation and coupling errors are reduced using differential spectroscopy [Fig. 9(b)], with the variance in calculated saturation using repeated measures on the same skin sample falling from 2.7% for absorbance to 1.5% for first differential and 1.3% for second differential spectroscopy.

For the human gastrointestinal studies, 804 measurements were performed in various segments of the gastrointestinal tract in 45 normal patients. Normal mucosal hemoglobin saturation (mean±SD) was 69±4%, while in tissue later determined to be tumors, this value was 45±23% ($n=14$, $p<0.0001$). The normal values were demonstrated to be normally distributed (Kolmogorov-Smirnov test of normal distribution for continuous variables, $p<0.005$). The tight variation in the normal values suggests that VLS oximetry is measuring reliably and reproducibly in tissue; the low oxygenation measured in human spontaneous gastrointestinal tumors suggests that VLS spectroscopy is sensitive to baseline tumor ischemia.

Table 1 Percent up time of T-Stat® oximeter versus pulse oximeter during cardiac surgery. Up time was calculated as percent of 5-s intervals during which at least one valid data point was recorded.

Bypass surgery clinical period	T-Stat® oximeter up-time (%)	Pulse oximeter up-time (%)
Start	100%	89%
Cooling	100%	32%
Cardiac arrest	100%	2%
Warming	100%	49%
Closing	99%	78%
End	100%	70%

For the human cardiac surgery studies, the up time of the system during various stages of cardiac surgery is shown in Table 1. The VLS oximeter had little down time during these studies. Unlike pulse oximetry, hand or body motion did not interfere with the ability of the VLS oximeter to collect spectral data, and to report oximetry results.

4 Discussion

We report a small probe or catheter clinical tissue oximeter based on visible light spectroscopy (VLS), and demonstrate quantitative measurement of hemoglobin saturation *in vivo* and *ex vivo*, sensitive to local ischemia. We term this approach VLS, analogous to the term NIRS, to emphasize that the benefits and drawbacks of visible light stem directly from the differing behavior of visible and near-infrared light in tissue. Validation of VLS oximetry in animal and human subjects is reported in a peer-reviewed companion medical article.[25] This VLS oximeter differs from prior *in vivo* tissue oximetry in two key ways.

First, a major advantage of VLS over NIRS is that it enables highly stable, small volume oximetry measurements in tissue, a key step in the development of spectroscopic, therapeutic catheters and probes. Visible light penetrates shallowly and locally in most tissues, even in the absence of hemoglobin. VLS tissue volumes are typically 125 μL or less, as compared to 30 ml or more for NIRS. This allows VLS to be incorporated into small needles and clips in a manner not feasible for NIRS. Localized measurements for tumor identification incorporating visible light have been used by Bigio et al.[47] and Mourant et al.[48] who term this elastic scattering spectroscopy. They measured and modeled light behavior using wavelengths as short as 280 nm to detect tumors. Bhutani et

al. used a combination of visible and near-infrared light to measure superficial bilirubin levels in skin (BiliCheck, SpectRx, Norcross, Georgia).[49]

Second, this study shows that use of VLS allows clinical oximeter probes to be formed into small probes, clips, internal catheters, or needles and deployed *in vivo*. In contrast to NIRS hemoglobin absorbance bands, which are relatively weak and flat, VLS solves for hemoglobin oxygen saturation using the blue to yellow spectrum (400 to 625 nm), wavelengths for which hemoglobin Q- and Soret-band absorbance is 2 to 3 orders of magnitude stronger than in the near-infrared. This strong visible light absorbance has been used for oximetry *in vivo* by other groups for large fiber bundle probes or noncontact cameras, including Lübbers and Wodick,[50] Jöbsis et al.,[51] Malonek and Grinvald,[52] Harrison et al.,[53] Feather et al.,[54] and Frank et al.[55]

With regard to reflectance standards, we now avoid liquid standards. Drawbacks of liquid standards include long-term changes in dispersion, variations between batches,[56,57] and the Mie-based intensity oscillations observed in this report, all of which make liquids difficult to validate as clinical reference standards. Liquid standards also present compatibility and safety issues when used with hollow catheters or injection needles. We prefer solid, diffuse-scattering, paper-based standards for the reflection probes and catheters, and a soft polysiloxane standard for the needle probes. Of note, dye standards such as quantum dots can be incorporated into the reflectance standard to provide wavelength calibration and volume of measurement benchmarks at the bedside.

Last, because VLS measures small, subsurface tissue volumes while NIRS measures larger, deeper volumes of tissue, VLS can answer different clinical questions than NIRS, and may in fact be complementary to NIRS. Clinical success has now been demonstrated for VLS in ischemia detection during vascular surgery, tumor ablation by radio-frequency ablation, gastrointestinal endoscopy, and other areas.[36,58–60]

Acknowledgments

Initial work was supported by the United Cerebral Palsy Foundation, Office of Naval Research (N-00014-91-C0170), and NIH/NINDS SBIR support to the Spectros Corporation (N43-NS-6-2313, and -2315). Work on the clinical oximeter was supported in part by CaP CURE (Peter T. Scardino, MD, PI, DAB co-P.I.).

References

1. K. Mathes, "Untersuchungen über die sauerstoffsättingungen des menschlichen arterienblutes [German]," *Arch. Exp. Pathol. Pharmacol.* **179**, 698–711 (1935).
2. M. S. Patterson, B. Chance, and B. C. Wilson, "Time resolved reflectance and transmittance for the non-invasive measurement of tissue optical properties," *Appl. Opt.* **28**, 2331–2336 (1989).
3. G. A. Milikan, "An oximeter: an instrument for measuring continuously oxygen saturation of arterial blood in man," *Rev. Sci. Instrum.* **13**, 434–444 (1942).
4. F. F. Jöbsis, "Noninvasive, infrared monitoring of cerebral and myocardial oxygen sufficiency and circulatory parameters," *Science* **198**(4323), 1264–1267 (1977).
5. E. M. Sevick, B. Chance, J. Leigh, S. Nioka, and M. Maris, "Quantitation of time- and frequency-resolved optical spectra for the determination of tissue oxygenation," *Anal. Biochem.* **195**(2), 330–351 (1991).
6. C. D. Kurth and W. S. Thayer, "A multiwavelength frequency-domain near-infrared cerebral oximeter," *Phys. Med. Biol.* **44**(3), 727–740 (1999).
7. W. N. Colier, N. J. van Haaren, and B. Oeseburg, "A comparative study of two near infrared spectrophotometers for the assessment of cerebral haemodynamics," *Acta Anaesthesiol. Scand., Suppl.* **107**, 101–105 (1995).
8. J. S. Wyatt, M. Cope, D. T. Delpy, S. Wray, and E. O. Reynolds, "Quantification of cerebral oxygenation and haemodynamics in sick newborn infants by near infrared spectrophotometry," *Lancet* **2**(8515), 1063–1066 (1986).
9. V. Quaresima, S. Sacco, R. Totaro, and M. Ferrari, "Noninvasive measurement of cerebral hemoglobin oxygen saturation using two near infrared spectroscopy approaches," *J. Biomed. Opt.* **5**(2), 201–205 (2000).
10. C. E. Elwell, S. J. Matcher, L. Tyszczuk, J. H. Meek, and D. T. Delpy, "Measurement of cerebral venous saturation in adults using near infrared spectroscopy," *Adv. Exp. Med. Biol.* **411**, 453–460 (1997).
11. R. E. Hayden, M. A. Tavill, S. Nioka, T. Kitai, and B. Chance, "Oxygenation and blood volume changes in flaps according to near-infrared spectrophotometry," *Arch. Otolaryngol. Head Neck Surg.* **122**(12), 1347–1351 (1996).
12. Y. Kakihana, A. Matsunaga, K. Tobo, S. Isowaki, M. Kawakami, I. Tsuneyoshi, Y. Kanmura, and M. Tamura, "Redox behavior of cytochrome oxidase and neurological prognosis in 66 patients who underwent thoracic aortic surgery," *Eur. J. Cardiothorac Surg.* **21**(3), 434–439 (2002).
13. See http://www.accessdata.fda.gov/scripts/cdrh/cfhdocs/cfpmn/pmn.cfm (Nov. 2004).
14. D. A. Benaron and D. K. Stevenson, "Optical time-of-flight and absorbance imaging of biologic media," *Science* **259**, 1463–1466 (1993).
15. J. P. van Houten, D. A. Benaron, S. Spilman, and D. K. Stevenson, "Imaging brain injury using time-resolved near infrared light scanning," *Pediatr. Res.* **39**, 470–476 (1996).
16. S. R. Hintz, D. A. Benaron, J. P. van Houten, J. L. Duckworth, F. W. H. Liu, S. D. Spilman, D. K. Stevenson, and W. F. Cheong, "Stationary headband for clinical time-of-flight optical imaging at the bedside," *Photochem. Photobiol.* **68**, 361–369 (1998).
17. D. A. Benaron, S. R. Hintz, A. Villringer, D. Boas, A. Kleinschmidt, J. Frahm, C. Hirth, H. Obrig, J. C. van Houten, E. L. Kermit, W. F. Cheong, and D. K. Stevenson, "Noninvasive functional imaging of human brain using light," *J. Cereb. Blood Flow Metab.* **20**(3), 469–477 (2000).
18. D. A. Benaron, C. Contag, and P. Contag, "Imaging brain structure and function, infection, and gene expression in the body using light," *Philos. Trans. R. Soc. London* **352**, 755–761 (1997).
19. C. H. Contag, S. D. Spilman, P. R. Contag, M. Oshiro, B. Eames, P. Dennery, D. K. Stevenson, and D. A. Benaron, "Visualizing gene expression in living mammals using a bioluminescent reporter," *Photochem. Photobiol.* **66**(4), 523–531 (1997).
20. C. H. Contag, P. R. Contag, J. I. Mullins, S. D. Spilman, D. K. Stevenson, and D. A. Benaron, "Photonic detection of bacterial pathogens in living hosts," *Mol. Microbiol.* **18**(4), 593–603 (1995).
21. D. A. Benaron, "Proposal to the opening a window into the human body: Development of a living biosensor allowing for improved monitoring of gene therapy, detection of infection, and more rapid drug development," Baxter Foundation, Stanford Univ. School of Medicine (1994).
22. D. Benaron, C. Contag, and P. Contag, founders of Xenogen (NASDAQ: XGEN) (1996).
23. M. Edinger, T. J. Sweeney, A. A. Tucker, A. B. Olomu, R. S. Negrin, and C. H. Contag, "Noninvasive assessment of tumor cell proliferation in animal models," *Neoplasia* **1**(4), 303–310 (1999).
24. T-Stat® ischemia detection system. Spectros Corporation, Portola Valley, CA.
25. D. A. Benaron, I. H. Parachikov, S. Friedland, R. Soetikno, J. Brock-Utne, P. J. van der Starre, C. Nezhat, M. K. Terris, P. G. Maxim, J. J. Carson, M. K. Razavi, H. B. Gladstone, E. F. Fincher, C. P. Hsu, F. L. Clark, W.—F. Cheong, J. L. Duckworth, and D. K. Stevenson, "Continuous, noninvasive, and localized microvascular tissue oximetry using visible light spectroscopy," *Anesthesiology* **100**(6), 1469–1475 (2004).
26. D. A. Benaron, B. Rubinski, S. R. Hintz, J. L. Duckworth, A. L. Murphy, J. W. Price, F. W. Liu, D. M. Otten, D. K. Stevenson, W. F. Cheong, and E. L. Kermit, "Automated quantitation of tissue compo-

nents using real-time spectroscopy," *Proc. SPIE* **3194**, 500–511 (1998).
27. D. A. Benaron, I. H. Parachikov, W. F. Cheong, S. Friedland, J. L. Duckworth, D. M. Otten, B. R. Rubinsky, U. B. Horchner, E. L. Kermit, F. W. Liu, C. J. Levinson, A. L. Murphy, J. W. Price, Y. Talmi, and J. P. Weersing, "Quantitative clinical nonpulsatile and localized visible light oximeter: design of the T-stat tissue oximeter," *Proc. SPIE* **4955**, 355–368, (2003).
28. "Excerpts related to EMI from November 1993 Anesthesiology and Respiratory Devices Branch," Document 628, U.S. Food and Drug Administration (1993) 75 pp.
29. International Standard IEC 60601-1, Medical Electrical Equipment, 2nd Edition, International Electrotechnical Commission (IEC), Geneva, Switzerland, 350pp.
30. European Medical Device Directive (MDD), Directive 93/42/EEC, Council of the European Communities Official Journal 1993; L-169(12/07/1993):1–43.
31. "Guidance for FDA reviewers and industry guidance for the content of premarket submissions for software contained in medical devices," U.S. Food and Drug Administration (1998).
32. "General principles of software validation: final guidance for industry and FDA staff," U.S. Food and Drug Administration (2002).
33. "Premarket notification 510(k): regulatory requirements for medical devices," Publication FDA 95-4158, U.S. Food and Drug Administration (1995).
34. J. Carson, P. G. Maxim, C. Hsu, I. Parachikov, and D. A. Benaron, "Optical detection of the cytotoxic drug tirapazamine in a mouse tumor model," *Med. Phys.* **30**(6), 1436 (2003).
35. D. Otten, B. Rubinsky, W. F. Cheong, and D. A. Benaron, "Ice front propagation in tissue using visible light spectroscopy," *Appl. Opt.* **37**(25), 6006–6010 (1998).
36. C. P. Hsu, M. K. Razavi, S. K. So, I. H. Parachikov, and D. A. Benaron, "Liver tumor gross margin identification and ablation monitoring during liver radiofrequency ablation using real-time visible light spectroscopy," J. Vascular Interven. Radiol. 2005 (in press).
37. D. A. Benaron and I. H. Parachikov, "Spectroscopy illuminator with improved delivery efficiency for high optical density and reduced thermal load," U.S. Patent 6,711,426 (2004).
38. W. G. Zijlstra, A. Buursma, and O. W. van Assendelft, *Visible and Near Infrared Absorption Spectra of Human and Animal Haemoglobin*, VSP Publishing, Utrecht (2000).
39. S. Prahl, http://omlc.ogi.edu/spectra/hemoglobin/index.html and www.spectros.com.
40. A. Roggan, M. Friebel, K. Dorschel, A. Hahn, and G. Muller, "Optical properties of circulating human blood in the wavelength range 400–2500 nm," *J. Biomed. Opt.* **4**, 36–46 (1999).
41. S. T. Flock, S. L. Jacques, B. C. Wilson, W. M. Star, and M. J. C. van Gemert, "Optical properties of intralipid: a phantom medium for light propagation studies," *Lasers Surg. Med.* **12**, 510–519 (1992).
42. C. D. Kurth, H. Liu, W. S. Thayer, and B. Chance, "A dynamic phantom brain model for near-infrared spectroscopy," *Phys. Med. Biol.* **40**(12), 2079–2092 (1995).
43. B. Tromberg, Beckman Laser Center, Irvine, CA; B. Balbieri at ISS, Urbana, IL; and D. Balbierz, Rita Medical Corporation, Sunnyvale, CA, Private Communications.
44. D. Boas, Department of Radiology, Massachusetts General Hospital, Boston, MA, Private Communication.
45. B. Chance, J. S. Leigh, H. Miyake, D. S. Smith, S. Nioka, R. Greenfeld, M. Finander, K. Kaufmann, W. Levy, M. Young, et al., "Comparison of time-resolved and -unresolved measurements of deoxyhemoglobin in brain," *Proc. Natl. Acad. Sci. U.S.A.* **85**(14), 4971–4975 (1988).
46. W. E. Weiser and H. L. Pardue, "Evaluation of multi-wavelength derivative spectra for quantitative applications in clinical chemistry," *Clin. Chem.* **29**(9), 1673–1677 (1983).
47. I. J. Bigio, S. G. Bown, G. Briggs, C. Kelley, S. Lakhani, D. Pickard, P. M. Ripley, I. G. Rose, and C. Saunders, "Diagnosis of breast cancer using elastic-scattering spectroscopy: preliminary clinical results," *J. Biomed. Opt.* **5**(2), 221–228 (2000).
48. J. R. Mourant, I. J. Bigio, J. Boyer, R. L. Conn, T. Johnson, and T. Shimada, "Spectroscopic diagnosis of bladder cancer with elastic light scattering," *Lasers Surg. Med.* **17**(4), 350–357 (1995).
49. V. K. Bhutani, G. R. Gourley, S. Adler, B. Kreamer, C. Dalin, and L. H. Johnson, "Noninvasive measurement of total serum bilirubin in a multiracial predischarge newborn population to assess the risk of severe hyperbilirubinemia," *Pediatrics* **106**(2), E17 (2000).
50. D. W. Lübbers and R. Wodick, "The examination of multicomponent systems in biological materials by means of a rapid scanning photometer," *Appl. Opt.* **8**(5), 1055–1062 (1969).
51. F. F. Jöbsis, J. H. Keizer, J. C. LaManna, and M. Rosenthal, "Reflectance spectrophotometry of cytochrome aa3 in vivo," *J. Appl. Physiol.: Respir., Environ. Exercise Physiol.* **43**, 858–872 (1977).
52. D. Malonek and A. Grinvald, "Interactions between electrical activity and cortical microcirculation revealed by imaging spectroscopy: implications for functional brain mapping," *Science* **272**(5261), 551–554 (1996).
53. D. K. Harrison, S. D. Evans, N. C. Abbot, J. S. Beck, and P. T. McCollum, "Spectrophotometric measurements of haemoglobin saturation and concentration in skin during the tuberculin reaction in normal human subjects," *Clin. Phys. Physiol. Meas.* **13**(4), 349–363 (1992).
54. J. W. Feather, M. Hajizadeh-Saffar, G. Leslie, and J. B. Dawson, "A portable scanning reflectance spectrophotometer using visible wavelengths for the rapid measurement of skin pigments," *Phys. Med. Biol.* **34**(7), 807–820 (1989).
55. K. H. Frank, M. Kessler, K. Appelbaum, and W. Dummler, "The Erlangen micro-lightguide spectrophotometer EMPHO I," *Phys. Med. Biol.* **34**(12), 1883–1900 (1989).
56. S. T. Flock, S. L. Jacques, B. C. Wilson, W. M. Star, and M. J. C. van Gemert, "Optical properties of intralipid: A phantom medium for light propagation studies, *Lasers Surg. Med.* **12**, 510–519 (1992).
57. H. G. van Staveren, C. J. M. Moes, J. van Marle, S. A. Prahl, and M. J. C. van Gemert, "Light scattering in intralipid-10% in the wavelength range of 400-1100 nanometers," *Appl. Opt.* **30**, 4507–4514 (1991).
58. S. Friedland, R. Soetikno, V. Gowra, and G. Singh, Presented at Digestive Disease Week Chicago, IL, June 2005.
59. J. Brock-Utne, E. S. Lee, A. Bass, F. R. Arko, J. Harris Jr., C. K. Zarins, P. S. van der Starre, M. K. Razavi, and C. Olcott IV, Presented at American Society of Anesthesiologists, New Orleans, LA, August, 2005.
60. P. G. Maxim, J. J. Carson, D. A. Benaron, B. W. Loo Jr., L. Xing, A. L. Boyer, and S. Friedland, "Optical detection of tumors in vivo by visible light tissue oximetry", Technol. Cancer Res. Treat. 2005 Jun;4(3):227–234.